

## **REVERSE FLOW PRESSURE LIMITING APERTURE (RF-PLA)**

Gerasimos D. Danilatos

ESEM Research Laboratory, 98 Brighton Boulevard, North Bondi, NSW 2026, AUSTRALIA

Telephone +61 2 91302837

Fax +61 2 93650326

Email esem@bigpond.com

*Running title:* REVERSE FLOW PLA

*Key words:* PLA, ESEM, SEM, environmental, differential, annular, aperture, supersonic, jet, pump.

## **Abstract**

The reverse flow pressure limiting aperture is a device that creates and sustains a substantial gas pressure difference between two chambers connected via an aperture. The aperture is surrounded by an annular orifice leading to a third chamber. The third chamber is maintained at a relatively high pressure that forces gas to flow through the annular aperture into the first of said two chambers. The ensuing gas flow develops into a supersonic annular gas jet, the core of which is coaxial with the central aperture. A pumping action is created at the core of the jet and any gas molecules leaking through the aperture from the second chamber are entrained and forced into the first chamber, thus creating a substantial pressure difference between the first and second chamber.

## **Introduction**

The transfer of charged particle beams from a low pressure region (vacuum) to a high pressure region through an aperture is achieved by means of differential pumping. Conventionally, this is done by maintaining one chamber at high pressure while a second chamber is pumped out at sufficient rate to remove the gas leaking through the connecting aperture which is known as pressure limiting aperture (PLA). Typically, the high pressure chamber may be around 1000 Pa while the low pressure one is around 10-20 Pa, so that the ratio of the two pressures is about two orders of magnitude.

In this paper, a novel method and apparatus has been tested and proposed for achieving pressure ratios of the same or greater order of magnitude between two chambers connected via an aperture. The principles of diffusion and Venturi vacuum pumps are applied to create a pumping action integrated with the PLA. Gas is supplied to the first chamber by a third chamber via an annular orifice around the PLA and the supersonic jet formed entrains and removes gas molecules out of the second chamber into the first.

Apart from the theory of diffusion pumps which create pressure ratios of several orders of magnitude in the very low pressure range, the Venturi principle both alone and in combination with the diffusion principle can be applied to operate in the intermediate and high pressure regimes. These regimes are of interest not only in particular applications such as those involving electron and ion beam technologies, but also in vacuum and gas dynamics technology, in general.

Langmuir (1916), Crawford (1917) and Alexander (1946) are some of the early pioneers of the theory and practice of vacuum pumps using mercury vapour. The vapour forms a supersonic expansion jet through various nozzles. The expanding vapour jet entrains the molecules that enter the jet via its periphery which communicates through an annular opening with the chamber under evacuation. The mercury vapour condenses by cooling means and re-enters the circulation. However, the vessel size and pressures used in those works are all outside the scope of the present system. The pumping takes place from the outside periphery of the annular jet formed with a condensable medium. It can be shown that the smallest variation in geometry can have a critical effect on the flow field and its pumping properties, especially in different pressure regimes and with different gases. At best, the integration of such techniques with a PLA constitutes only a desirable speculation at the outset.

A more recent publication has reported on the pumping properties of the interior of a supersonic ring-shaped gas jet (Ermolov et al., 1985). In that paper, the theories on pumping mechanisms have been critically surveyed and a set of experimental results presented. However, the vacuum levels predicted and achieved were very poor for our present purposes. For example, from the plots of pressure at the core vs. pressure at the downstream output, we see a compression ratio of only 1.33 which is unacceptable for a PLA as used in our context.

Several years of work and investigations by the present author have fortunately gone beyond this limit and shown the possibility of constructing a PLA with substantial pressure ratios,

namely, exceeding two orders of magnitude. The main purpose of this paper is to announce the new technique and to show its feasibility both by the direct simulation Monte Carlo method and by experiment. The more complex aspects of this system will be the subject of future reports.

### **Direct simulation Monte Carlo method.**

An annular jet capable of creating pressure ratios greater than one and usually greater than two or three orders of magnitude between its core and the downstream region into which it exhausts and which is held typically in the range of 100-1000 Pa has been hitherto unknown. A system with such an annular jet surrounding an aperture has not previously been made or used to create a sharp pressure gradient along the axis of the aperture through which two regions of substantially different pressures communicate. The lack of such a system may be attributed to the lack of a theory capable of dealing with the complex situation of gas flow in these pressures. Gas dynamics theories are very well developed either for the case where the mean free path is much larger than the vessel size (free molecular flow), or where the mean free path is much smaller than the size of the vessel (continuum flow). However, our system uses pressures which, in addition, include the transition and slip flow regime, and its behaviour has been theoretically unpredictable. The lacking information on such a system in the past may also be attributed to the lack of many instruments requiring a pressure differential with sharp pressure gradients. The advent of a commercial ESEM has created the need for significant improvements in this area.

The direct simulation Monte Carlo (DSMC) method overcomes these difficulties. This technique, as developed by Bird (1995) over several decades, has given a new impetus to revisiting gaseous flows impossible to satisfactorily study by other means. The recent availability of fast personal computers which can be devoted to solving a particular gas flow configuration over some hours, or even days, has made this method most practical. The DSMC method

models a real gas by many thousands, or even some millions, of simulated molecules in a computer. The velocities and positions of these molecules are stored in the computer and modified with time as the molecules are followed through their collisions and boundary interactions in simulated physical space. These programs were originally developed for use in space technology for relatively large flows and low pressures, but they have been adapted and found to also apply for the much smaller dimensions and large pressures used around a PLA (Danilatos, 1991).

The presently proposed system can be better understood with reference to Fig. 1. The device comprises chamber 1 held at pressure  $p_1$  (also referred to as specimen chamber, or ch1), chamber 2 held at pressure  $p_2$  (also referred to as PLA chamber, or ch2) and chamber 3 held at pressure  $p_3$  (also referred to as input chamber, or ch3). The system is axially symmetric around an axis 4. Chamber 1 communicates with chamber 2 via an aperture 5 (the PLA) defined by an inner nozzle 6. Chamber 1 also communicates with chamber 3 via an annular orifice 7 defined between an inner nozzle 6 and an outer nozzle 8. Chamber 3 is maintained at a higher pressure than chamber 1 so that gas can flow from 3 to 1. The annular gaseous flow formed, after it passes the throat of the annular orifice 7, expands and forms a supersonic annular jet 9 inside chamber 1. Gas is removed from chamber 1 by an appropriate pump and the pressure level can be regulated to a desired level. The supersonic jet eventually collides with the background gas of the chamber and a steady state flow is established. Under such conditions, the central region of the gaseous jet continuously entrains any gas molecules that pass through the PLA 5 from chamber 2. As a result, chamber 2 is continuously pumped out by the supersonic jet flow and a low equilibrium pressure is achieved in chamber 2. In this way, a pressure difference is established between chambers 1 and 2. Generally, gas tends to flow from chamber 2 to chamber 1 (i.e. in reverse direction relative to conventional technique of differential pumping), but at the equilibrium situation the direction of the net flow through PLA depends on how the pressure of chamber 2 is controlled. The direction of flow will go the other way when chamber 2 is maintained by an independent pump at a pressure below the level sustainable by the annular jet mechanism. If chamber 2 is sealed off and there is no leak

or outgassing in it, then the net gas flow through PLA is zero at the steady state situation. The term reverse flow pressure limiting aperture (RF-PLA) has been thought to reflect the contrasting situation relative to the conventional PLA, where the flow takes place always in the direction from chamber 1 to chamber 2 and where a gas plume is formed in the low pressure chamber (i.e. "above" the PLA). In an electron microscope, chamber 1 corresponds to the specimen chamber, chamber 2 to the electron optics above the PLA and chamber 3 is a new feature for the supply of input gas to the supersonic annular jet.

A large number, in fact, several hundred cases, of different geometries and boundary conditions have been tested with the DSMC program by this author in the span of several years. The approach has been semi-empirical in selecting the boundary conditions of the flow, but some practical rules have been deduced in this approach. It is not appropriate to present all the cases tested in this paper, and only some results showing the salient features of the flow are given below. All tested cases may have to be included in a special engineering report in order to avoid duplication of the same computations by other workers.

Initially, a geometry was tested which was close to that reported by Ermolov et al. (1985) and is shown in Fig. 2. Because the flow is axially symmetric, only the semi-plane on one side of the axis is shown, the axis oriented horizontally and both axial and radial dimensions drawn to scale in mm. The annular orifice is defined by converging and diverging surfaces of revolution formed by straight line segments around the axis. Argon is used with input pressure  $p_3=10$  kPa and chamber pressure  $p_1=400$  Pa. The gas flow after passing the throat of the annular orifice expands and forms a supersonic jet which results in a compression region in chamber 1 with maximum pressure  $p_m=1000$  Pa and a rarefaction pressure  $p_2=350$  Pa in the PLA region as shown in the figure. The contours represent equal increments of pressure. In this series of tests, the PLA is closed off with a surface integrated with the inner nozzle. Here, it is assumed that the presence for this surface does not affect the pumping mechanism of the annular jet. The average low pressure calculated at the surface is thought to represent the ultimate value of pressure for a large vessel which would freely communicate through an open PLA with the

specimen chamber. Therefore, the ratio of pressures between the specimen chamber and the PLA is a measure of the pumping efficiency for a given set of boundary conditions. We may consider either the ratio of the background pressure of the specimen chamber over the PLA pressure (i.e.  $p_1/p_2$ ), or the ratio of the maximum compression pressure in the specimen chamber over the PLA pressure (i.e.  $p_m/p_2$ ). Correspondingly, we have  $r=1.14$  and  $r_m=2.86$  for the case in Fig. 2, which is close to the Ermolov et al. reported result. However, these values are considered unacceptable for the purposes of the present innovation.

Nozzles with a combination of spherical, elliptical and straight line geometries have been tested producing different degrees of success. Because of the large number of variables, the first round of tests was laborious and time consuming but it produced some firm trends and conclusions: (a) Pressure ratios up to two orders of magnitude were achievable; (b) For a given boundary geometry and back-pressure in specimen chamber, the PLA pressure was strongly dependent on the variation of input pressure, namely, it showed a pronounced minimum value as we vary the input pressure; (c) For a fixed nozzle geometry, the PLA pressure showed a pronounced minimum as we shift the inner nozzle relative to the outer nozzle along its axis.

Both because straight line geometries showed good performance and because they are easier to effect in practice, a new series of tests were concentrated on such geometries. Furthermore, it was decided to use the leak rate of molecules through an open PLA as a measure of performance instead of the pressure at a sealed-off PLA described before. As the DSMC program produces a direct reading of the leak rates through interfaces, it was thought that it is safer to avoid a surface that might perturb the gas flow, especially in cases where the supersonic region does not cross the axis of the PLA. The leak rate is given in molecules per second (mols/s) after the steady state flow is achieved, and can be compared with the leak rate of a flow field having the same back-pressure in the specimen chamber but without the region 3 supplying gas, which is equivalent to setting  $p_3=p_1$ . For example, with  $p_3=p_1=100$  Pa and PLA exhausted in vacuum, we find the reference leak rate through PLA to be  $Q_0=583 \times 10^{15}$

mols/s. Fig. 3 shows the leak rate of argon vs. input pressure for the geometry that accompanies the curve, at fixed  $p_1=100$  Pa and fixed position of inner nozzle (PLA radius is 0.25 mm with all other dimensions drawn to scale). At the minimum value of the curve, we get an optimum leak rate ratio of  $583 \div 1.5 = 389$ . Fig. 4 shows a slightly different geometry for the outer nozzle and the accompanying graph shows the variation of leak rate of argon vs. axial shift of the inner nozzle at fixed  $p_1=100$  Pa and  $p_3=15$  kPa. The optimum leak rate ratio is  $583 \div 1.34 = 435$ , which is an excellent result. At the optimum position of inner nozzle, the flow field with isodensity contours (in mols/m<sup>3</sup>) is presented in Fig. 5. The line of sonic surface containing the supersonic region, seen in the same figure as a thick line, crosses the axis of the aperture so that no gas from the specimen chamber can diffuse back through the PLA. At the shock wave where the jet meets the background gas of the specimen chamber, the maximum pressure is about 130 Pa. It can be shown that this maximum varies both in intensity and in distribution, as we shift the inner nozzle, in a manner analogous to the variation of a water jet from a garden hose sprinkler by shifting the spindle along the axis of the sprinkler (i.e. the jet becoming spread out, or focussed on the axis).

These computational tests show that it is possible to use the proposed system for creating substantial pressure differentials with one, two and three orders of magnitude pressure ratios which can be used in many applications without further modifications. However, it may be desirable in some applications to maintain a specimen in an environment of uniform pressure, i.e. without a compression effect in the proximity of the specimen, a condition which can be achieved by the following solutions: (a) We place the specimen at sufficiently long distance from the action of the jet; (b) If the specimen has to be placed as close as possible to the PLA, then the inner nozzle can be shifted in a direction that spreads the jet outwards in a more or less uniform distribution; (c) If the latter distribution is still not satisfactorily uniform for some applications, while also the pumping efficiency may be compromised, a radical solution is achieved by the use of baffles. A baffle is a solid surface that intercepts the jet before it strikes the specimen. One practical and effective baffle is a thin plate with an orifice coaxial with the PLA. In electron optical instruments, it is preferred to have such an orifice larger than the



PLA in order to allow unlimited field of view. It is also preferred to position the baffle at as close range to the PLA as possible in order to minimise the electron beam travel in the high pressure region. A practical configuration is shown in Fig. 6 where a baffle is placed 1.5 mm and the specimen 2.0 mm from the throat of the annular orifice. A complete drawing for the same system is also shown in Fig. 12. The inner nozzle has been shifted to its optimum position on the axis, corresponding to the minimum on the curve of leak rate  $Q$  vs. shift also shown in Fig 6. By plotting the flow-lines of the field, we see that practically all of the gas is diverted in the region between baffle and outer nozzle, so that the surface of the specimen experiences the uniform stagnant conditions of the specimen chamber. At this condition, the specimen chamber pressure equals the total jet pressure which is the sum of static plus dynamic pressure in it. The region between baffle and outer nozzle is pumped out by a mechanical pump, in this case, the pressure  $p_4$  at its inlet being 20 Pa. By such means, we may actually use a different gas in the specimen chamber from that used in the pumping jet. Therefore, the specimen chamber and the electron optics column can be totally separated by this approach. Water vapour, or any other gas can be introduced in the specimen chamber while an inert or non-contaminant gas can be used for the jet. This is a fundamentally novel technology for separating two regions freely communicating with each other via an open aperture along the axis of which there are sharp pressure gradients separating different pressures and, even, different gases.

It should be noted that the parameter of temperature can also play a critical role in the pumping efficiency of the apparatus. All the examples shown use room temperature ( $T=293$  K) at the boundaries of the flow field. Higher and lower temperatures have also been tested. As a general rule, high temperature at the input gas generally increases the efficiency because the energy of the driving gas is higher. There is a number of combinations of temperatures at various boundaries but the large volume of results obtained cannot be discussed in this report.

## **Experimental**

While the DSMC method has been proven to be very reliable, it is pertinent to eventually design and construct an experimental apparatus not only to verify the above findings but also to extend the measurements into regimes which would require very long computational times even with the latest personal computers. A versatile experimental apparatus, which includes a baffle, has been used as shown in Fig. 7.

For future reference and evaluation of the results the apparatus is described in detail: A length of 4.2 mm from a hypodermic needle with 0.6 mm outside diameter and 0.4 mm inside diameter was obtained. One end of the needle segment was widened to have 0.5 mm inside diameter and the outside edge was tapered from the outside face at about 45 degrees angle. The other end was sealably fixed at the 0.6 mm hole of a commercially supplied thin copper grid which, in turn, was sealably fixed at the rim of a metal pipe having 3 mm inside diameter and 100 mm length. A flexible hose connected the free end of the metal pipe to a McLeod gauge shown as PG2 in Fig. 7. The metal pipe was fixed vertically to a system of electronically driven micromotors so that the needle can be shifted in the x, y and z direction with an accuracy better than one micron while the position is digitally displayed. The needle (i.e. the inner nozzle) moves inside a 0.8 mm hole of a commercially supplied thin copper grid (i.e. the outer nozzle) being fixed via a wider plate on to the top of a 10 mm diameter and 50 mm long metal tube which communicates with and is fixed to a larger vessel containing the micromotors. The latter vessel termed chamber ch3 can be evacuated and its pressure regulated via a gas inlet leak valve (LV) at any pressure between 0-100 kPa and monitored with a combined mercury manometer and a McLeod gauge (PG3). A smaller cylindrical vessel (40 mm diameter) with two compartments, namely, ch1 and ch4, has a coaxial hole with an o-ring so that it can sealably move to vary the distance d. Chamber ch1 is 20 mm high and communicates first with an electronic absolute pressure meter (PG1) on its side wall and second with ch4 via a hole of 2 mm diameter on a thin plate acting as baffle. Chamber ch4 is directly evacuated with a rotary pump and its pressure monitored with a McLeod gauge attached to its side wall (PG4). The distance between baffle and outer nozzle can be varied

from near zero to more than 10 mm. The baffle hole together with the PG1 gauge effectively act as a Pitot system measuring the total (static plus dynamic) pressure of the flow. Similarly, the needle effectively measures the static pressure, at its tip, of a gas flow usefully and deliberately perturbed by the needle itself. The needle tip can move at both "below" (say, negative) and "above" (say, positive) positions relative to the outer nozzle. The flat top wall of ch1 was made from glass to allow viewing with a stereoscope. The purpose of optical viewing was initially to allow best centering of the needle and setting a zero reference position. However, optical viewing proved more valuable than that, as possible condensation of the expanding gas could also be monitored. A drying agent (silica gel) was used at the input of the leak valve admitting gas into chamber ch3, in order to remove moisture that, being condensable, could falsify the McLeod readings. Different gases have been tested such as air, nitrogen and water vapour. The temperature of the input gas could also be raised with a heating element.

The above described apparatus proved most versatile for a series of varied experiments. Only some representative results obtained with dry air are presented below. Measurements were obtained as follows: The baffle and needle position being fixed, the pressure of chamber ch3 was varied and all corresponding pressures, namely  $p_1$ ,  $p_2$ ,  $p_3$  and  $p_4$ , recorded. Then, the needle only was shifted to a new position by a small distance (i.e. 10, 20, or 50 microns) and the measurement of pressures repeated by varying the input pressure. A further series was repeated for a new position of the baffle, and so on. A general idea of the behaviour of the system can be obtained by plotting the contours for  $p_2$  on a shift/ $p_1$  plane as shown in Fig. 8. This is done for the case of baffle distance being 2 mm. The contours show the dependence of  $p_2$  on both needle position and specimen chamber pressure at the different increments of  $p_2$  shown with each contour. We clearly see that the lowest  $p_2$  pressures are recorded for positive shifts around 100 microns for all  $p_1$  pressures. This means that the inner nozzle can be put at a fixed position giving best pumping regardless of specimen chamber pressure. A small only adjustment of shift can improve the efficiency, but for practical purposes this may not be necessary. From the same set of measurements, we plot  $p_2$  vs.  $p_3$  at fixed needle positions (in

microns) shown with each curve in Fig. 9. We also plot  $p_2$  vs. nozzle shift at fixed  $p_1$  values shown with each curve in Fig. 10. By these plots, we confirm the predicted trend and order of magnitude of pressures previously obtained by the DSMC calculations.

The case where the baffle was positioned at 2 mm distance from the throat of the annular orifice was studied in more detail including negative positions (i.e. needle tip "below" the outer aperture). Baffle positions at 3, 4 and 5 mm were also studied but the measurements were concentrated around the optimum performance points in order to establish the highest pressure ratios with the given geometry. Fig. 11 shows the pressure ratios ( $p_1/p_2$ ) around those optimum conditions for the four cases of baffle distance (in mm) indicated with each curve. Clearly, at the longer baffle distance the efficiency is highest reaching values greater than 500. The behaviour of these measurements can be better understood in the light of the finding described below:

The experiments have revealed a rather unexpected phenomenon. It has been found that, as we raise the ch3 pressure, ch1 pressure first rises and ch2 pressure falls accordingly, but we reach a point at which the ch1 pressure falls abruptly. At this point, we have to raise the ch3 pressure by a large amount in order to restore the previous ch1 value and continue beyond it but, by then, ch2 pressure is also raised abruptly and the corresponding pumping efficiency becomes poor. This phenomenon is reproducible and shows a particular trend as we vary the conditions. The points of onset of this transition, or breakdown, are shown by a thick line in Fig. 8. It is thought that this phenomenon may be attributed to a transition from smooth to turbulent flow causing a serious back-flow of gas through the needle into ch2 and it may also be connected with the shape of sonic surface shown in Fig. 5. This phenomenon may correspond to a transition of the annular jet from a focussed to a spread condition. The optical observation of the system during testing also revealed that there is liquefaction of the expanding gas because condensation is seen around the outer rim of the needle and on the outer nozzle. This condensation was present even with dry nitrogen, or air and it seemed to reach a steady state whereby the liquid phase does not increase beyond a small amount

deposited on the said surfaces. These droplets did not seem to cause the onset of the transition, as very high pressure ratios were recorded in their presence. Most importantly, however, it has been found that by raising the temperature of the input gas by about 20<sup>o</sup> C, we can obtain much higher pressure ratios, and the point of transition is shifted to higher specimen chamber pressures. Thus, pressure ratios up to three orders of magnitude have been recorded. Also, specimen chamber pressures could be greater than 700 Pa while  $p_2$  was below 70 Pa even after the breakdown occurred. A systematic study of the transition mechanisms and the temperature effect continues at present.

## **Discussion**

The purpose of this paper is to make a preliminary announcement on the RF-PLA and the results reported by no means constitute the best situation achievable. The boundary conditions shown do not represent a unique solution. The optima presented are only partial solutions and further research will establish which one of similar solutions is best (optimum optimorum).

Based on the results of this work, the principle described by Fig. 1 can be used also in vacuum technology to improve the ultimate vacuum achieved by mechanical pumps. At this stage, an improvement of vacuum seems possible at least when the vessel under evacuation is small and the pumping speed required is low. With further research, it is anticipated to increase both the vacuum level and the pumping speed.

In instruments where a specimen is introduced in chamber 1, the presence of a gas jet impinging on the specimen may be beneficial, irrelevant or detrimental. In the latter case, a few different solutions are available and the introduction of a suitable baffle provides a radical option. For better understanding, the system corresponding to Fig. 6 is fully drawn to scale in Fig. 12. A pump evacuates chamber ch4 which is generally maintained in rough vacuum of say 20-100 Pa and, therefore, the type of pump required is only with a good throughput

specification. The same pump can be used to regulate the specimen chamber (ch1) pressure normally via the baffle orifice, although its inlet can also be shunted directly to the specimen chamber. The specimen chamber can be supplied with the same gas used in chamber ch3, or it can be independently supplied via an inlet leak valve with a different gas. The latter gas can be made to slightly "overflow" and mix with the jet gas in chamber ch4, or it can be made to "underflow" and mix with the gas jet in chamber ch1. These and other combinations are possible and desirable in various applications.

Instead of baffles, we may use skimmers as used in molecular beam technology (e.g. Bier and Hagena, 1963). A skimmer achieves the opposite effect to a baffle. It removes the peripheral fraction of gas from a supersonic jet while it allows only the core fraction to be transmitted through the orifice of the skimmer. It is now proposed that the annular jet can be used as a source of a very intense core of gas jet which can be skimmed by known techniques of related technologies.

Care should be taken in the design of the system because the number of configurations of geometry and other boundary conditions producing a practical result are much less than those which do not. In this context, it is useful to recall that, for a given working situation, there is a corresponding locus of mechanically similar flows which can have a practical application.

We have obtained good qualitative and semi-quantitative correspondence between experiment and DSMC calculations. We do not have one to one quantitative correspondence between experiment and DSMC for the cases reported because the exact geometries predicted could not be exactly reproduced by the resources presently available to this author. However, a careful measurement of the experimental geometry used can, conversely, be tested by the DSMC method, but this is left for later academic work. The veracity of the DSMC method has been tested on simpler systems and the verification of the present invention by an experimental apparatus has placed the system on good foundations.

The present innovation produces several advantages when it is integrated with electron optical systems. The integration of the RF-PLA with electron optics systems can be most readily achieved. In fact, various parts of the RF-PLA ideally lend themselves to function as parts of the electron optics and detection system. For example, the inner and outer nozzles and baffle can be used as detection electrodes, shield electrodes and focussing electrodes.

The RF-PLA allows the use of improved electron optics and field of view by eliminating the need of a second PLA along the beam path, in the low pressure region, as is currently practised and which limits the field of view at the very low magnifications. This means that the RF-PLA should be placed as close as possible to the "rocking point" of an electron beam in an ESEM, which will allow the restoration of full field of view as in the vacuum SEM.

The specimen chamber can be continuously fed with a gas stream directly impinging on the specimen under examination. It is now possible to effect a quick change of gas at the specimen surface by properly controlling chamber 3. This can be an advantage in ion beam technology, in micro-fabrication, in micro-electronics industry and certain applications in electron/ion microscopy. Gases can be more effectively delivered for metal deposition, or chemical etching.

The back-flow of impurity gases (e.g. by outgassing specimens and oil pumps) from the specimen chamber into the electron optics chamber is practically eliminated, or minimised. This is an advantage in electron microscopes and ion beam instruments where the electron optics must be protected from deleterious contaminants and only clean gases may be allowed to leak through. As a further consequence, the separation and protection of the electron optics column has also the advantage that any gas can be used that may improve the performance of the gaseous detection devices used in ESEM. For example, various quenchers that increase the gain of the detector can now be used without fearing the deleterious effects that some of these gases can have in the electron optics column.

The charged beam suffers significantly less particle losses by way of collisions as the beam is transferred from chamber 2 to chamber 1. This advantage is due to the fact that the mass thickness in the transition region of the present device is less than the corresponding mass thickness in the transition region of conventional PLA. In a conventional PLA, the gaseous plume above the aperture is responsible for a significant loss of electrons, while in the present method such a jet is absent with a concomitant depletion zone below the aperture. This advantage becomes significant in charged beams of low energy and gases with high scattering cross-sections. There is a significant number of applications where this advantage is applicable.

No pump is needed to evacuate chamber 2 which is compulsory for conventional differential pumping. In systems where already one other pump is devoted to pumping and regulating the specimen chamber, it is now possible to work with one pump less. The elimination of one intermediate pumping stage results in reducing production and operational costs for the instrument, in saving useful space and in reduced noise.

Of no less significance, the new invention (Danilatos 1999) provides alternative means for differential pumping to existing technologies, which allows for more diverse and competitive industries.

## **Conclusion**

A new approach to differential pumping technique has been shown. An annular gas jet is formed around a pressure limiting aperture, ejecting gas in the direction of the specimen chamber. A rarefaction created at the core of the jet results in pumping action which removes gas through the aperture and creates a substantial pressure difference across the two sides of the aperture. This can be used to separate the vacuum of the electron optics column from the high pressure in the specimen chamber of an instrument.



## **Journal Articles**

Alexander P (1946) The theory of the mercury-vapour vacuum pump and a new high-speed pump. *J. Sci. Instrum.* 23:11-16.

Bier K and Hagena O (1963) Influence of shock waves on the generation of high-intensity molecular beams by nozzles. *Rarefied Gas Dynamics* 1:478-496. Academic Press, New York, Ed. Laurmann J.

Crawford WW (1917) The parallel jet vacuum pump. *Phys. Rev.* 10:557-563.

Danilatos GD (1991) Gas flow properties in the environmental SEM. *Microbeam Analysis-1991*:201-203. San Francisco Press, Ed. Howitt DG.

Danilatos GD (1999) Differential pumping via core of annular supersonic jet. WIPO, PCT patent application, Intern. Publication Number WO 99/27259, 3 June 1999.

Ermolov VI, Kusner YS and Prikhod'ko VG (1985). Structure and pumping properties of the inner portion of a supersonic ring jet. *Sov. Phys. Tech. Phys.* 30(1):105-111.

Langmuir I (1916) A high vacuum mercury vapour pump of extreme speed. *Phys. Rev.* 8:48-51.

## **Books**

Bird GA (1995) *Molecular Gas Dynamics and the Direct Simulation of Gas Flows*. Oxford: Clarendon Press.

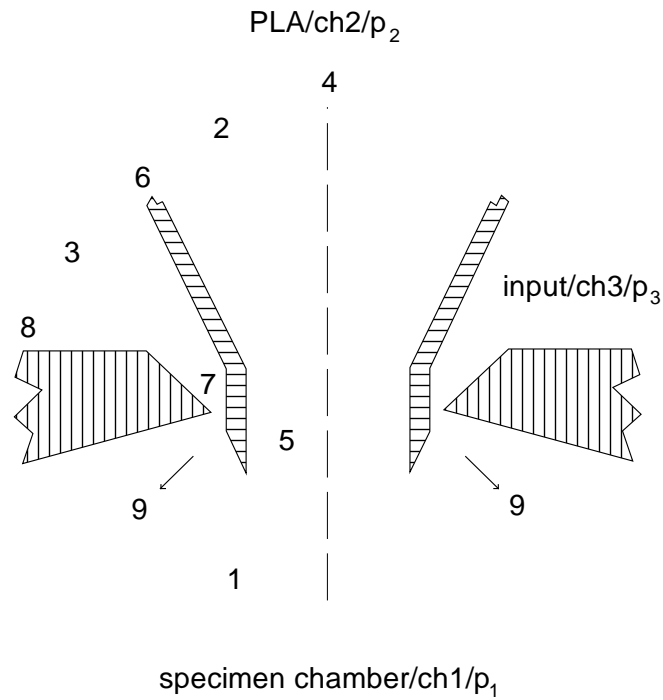


Fig. 1 Principle and schematic of the reverse flow pressure limiting aperture: Inner nozzle 6 with coaxial outer nozzle 8 form annular orifice 7 around central aperture 5 and system axis 4. Gas flows from input chamber 3 (ch3) at pressure  $p_3$ , into chamber 1 (ch1) at pressure  $p_1$ , forming annular gas jet 9 with core pumping action which results in low pressure  $p_2$  in chamber 2 (ch2) whereby  $p_2 \ll p_1$ .

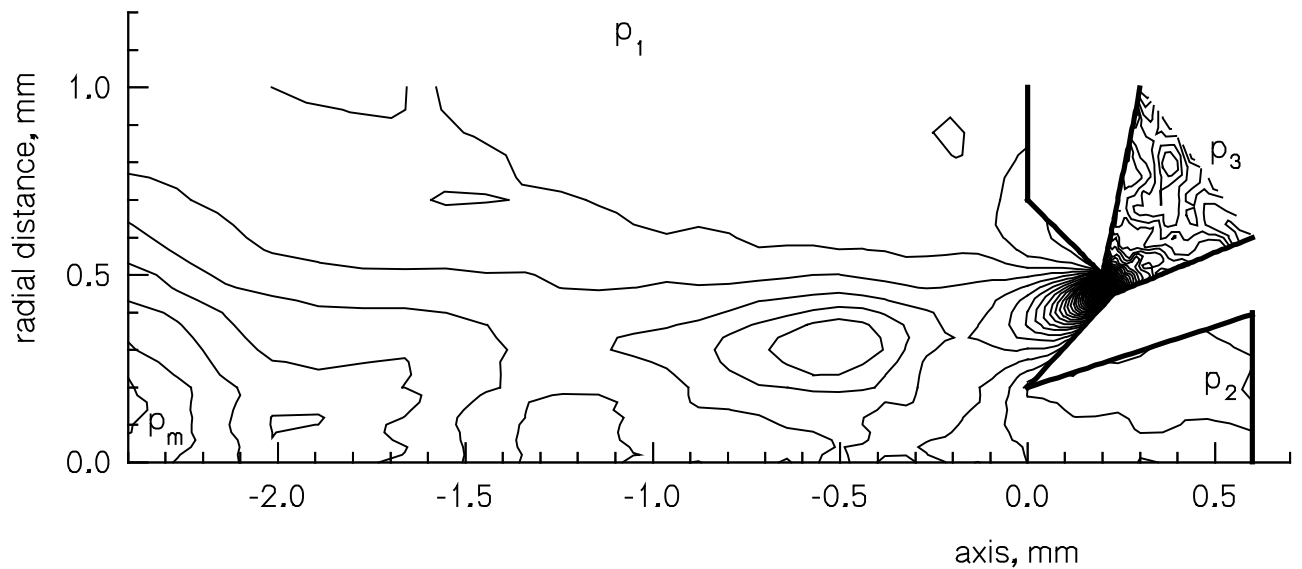


Fig. 2 Isodensity contours around an axis for argon supplied at input pressure  $p_3$  and exhausting via annular orifice into specimen chamber at pressure  $p_1$  while it creates a compression maximum pressure  $p_m$  in the chamber and rarefaction pressure  $p_2$  at PLA.

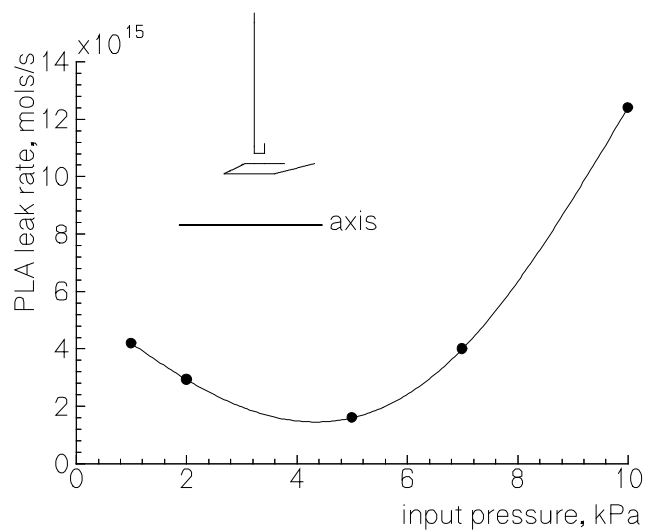


Fig. 3 Variation of leak rate through PLA vs. input pressure for the fixed geometry shown.

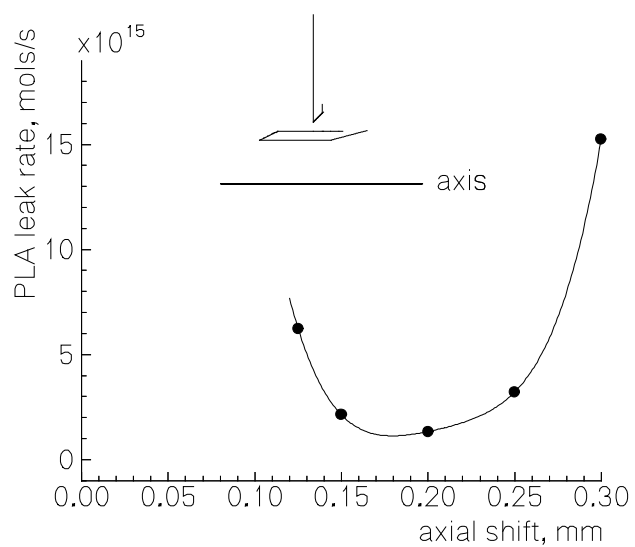


Fig. 4 Variation of leak rate through PLA vs. axial shift distance of the inner nozzle of the geometry shown.

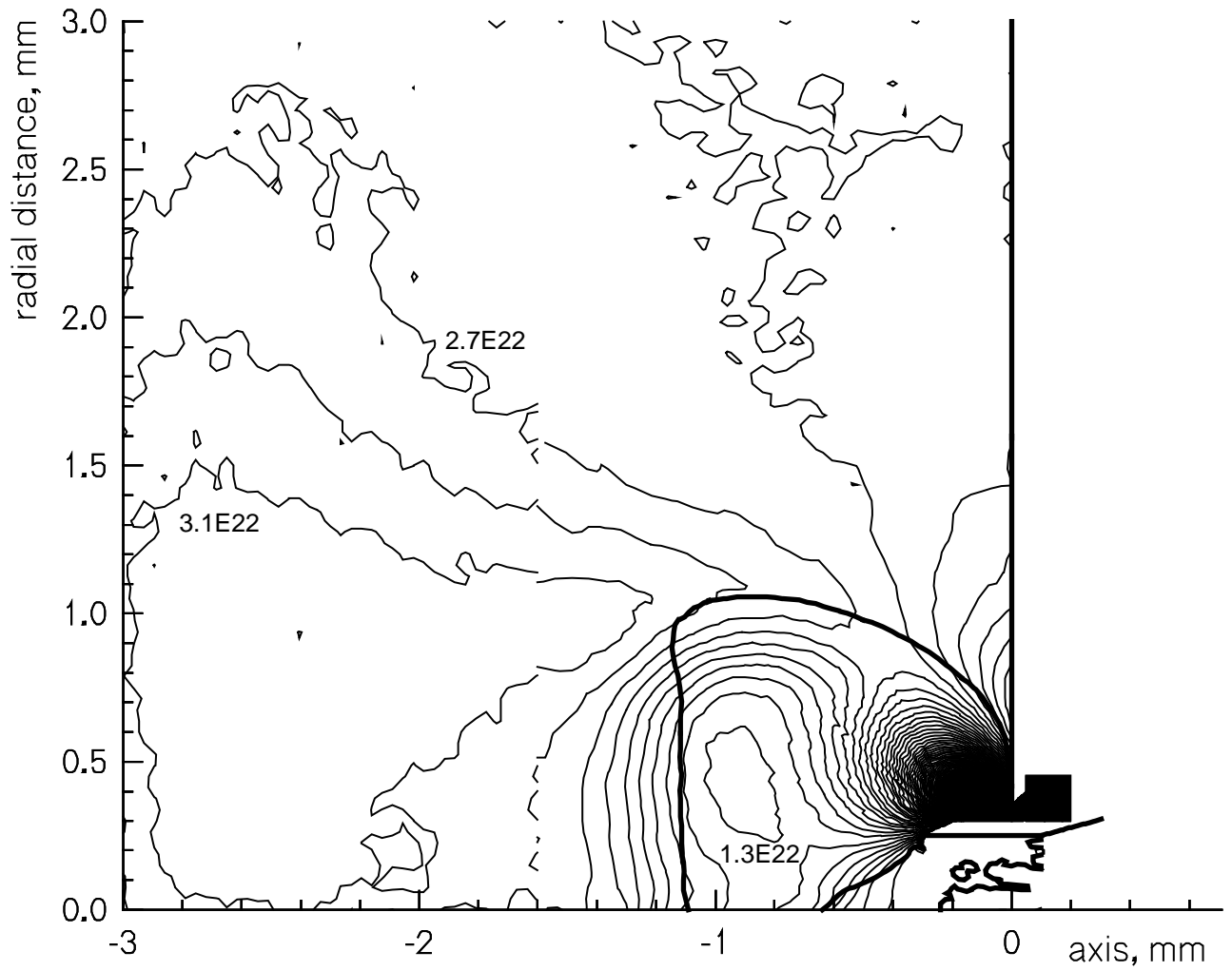


Fig. 5 Isodensity contours in  $\text{mols/m}^3$  at equal increments and sonic surface (thick line) at the optimum location of the inner nozzle.

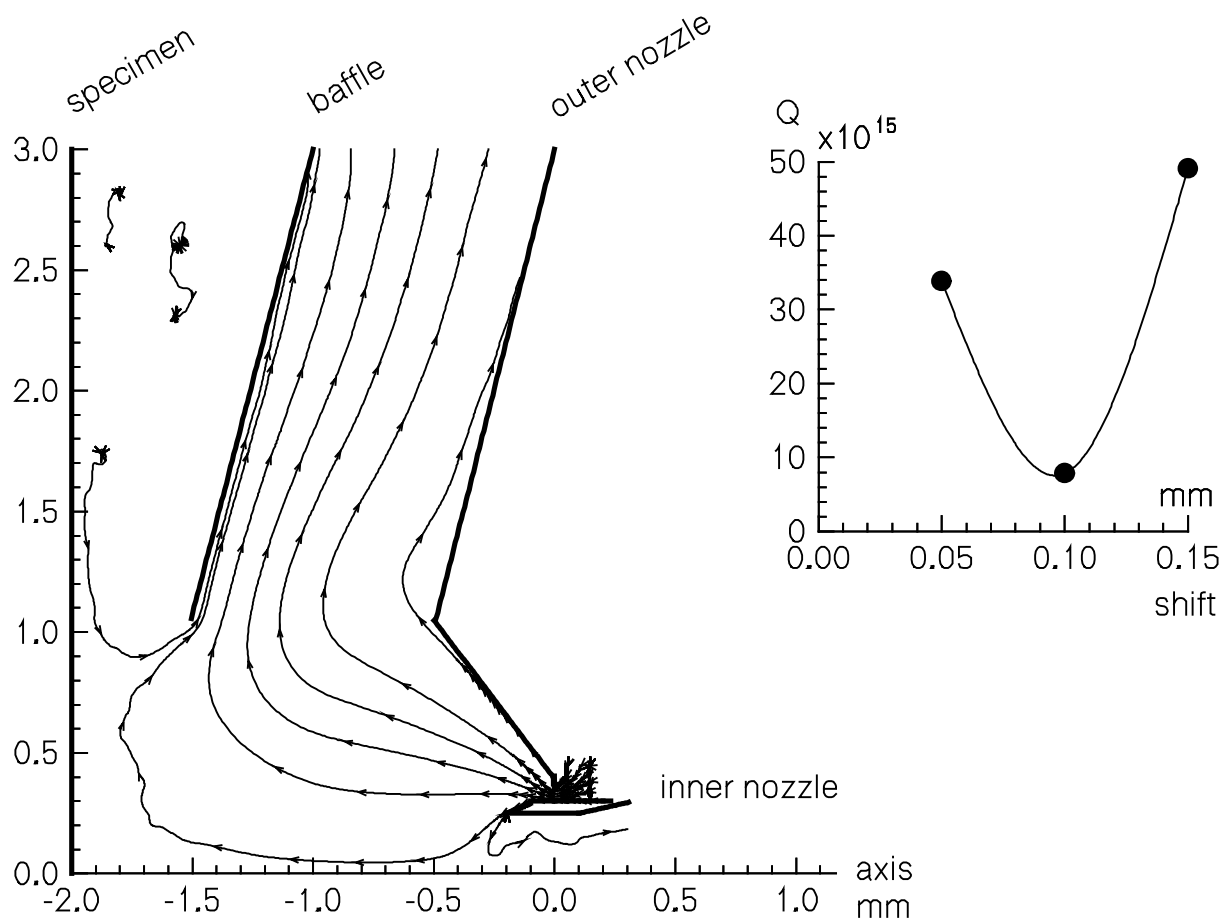


Fig. 6 Flow lines of RF-PLA system with baffle and specimen downstream of the annular jet flow. Inner nozzle is positioned at the point of minimum leak rate  $Q$  vs. axial shift shown in the upper right corner graph drawn in the fashion of Fig. 4.

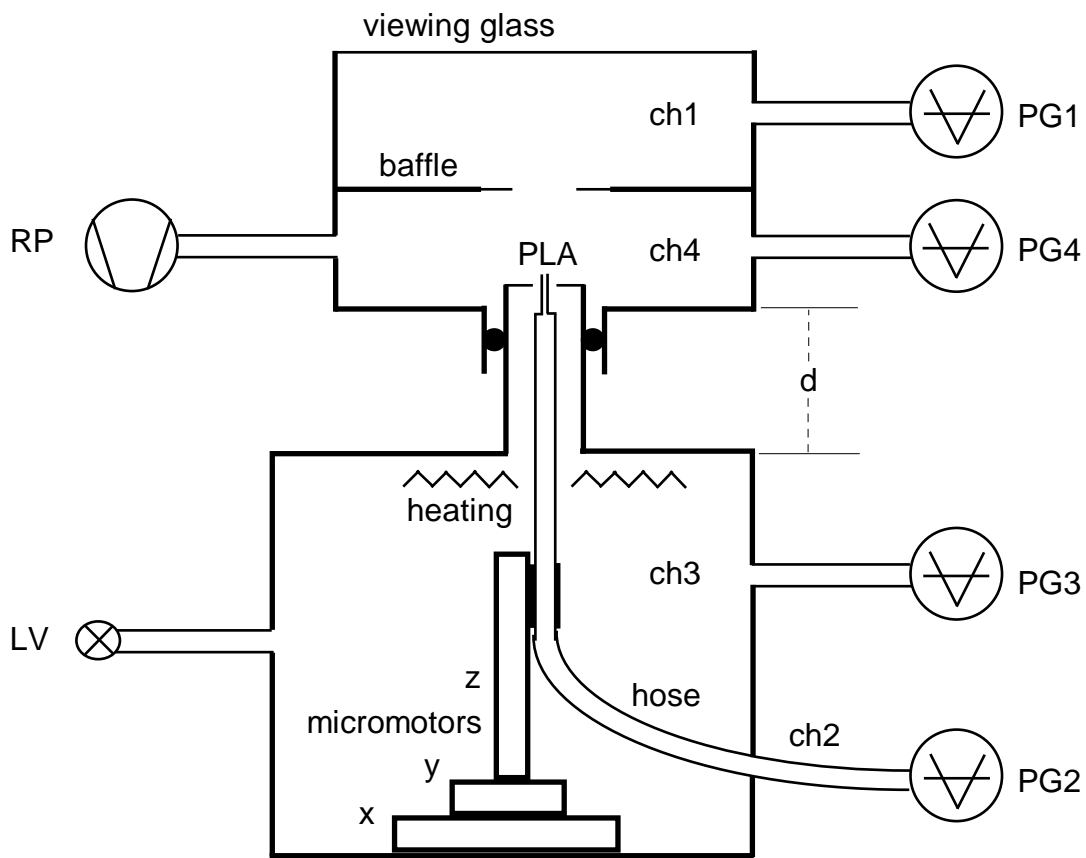
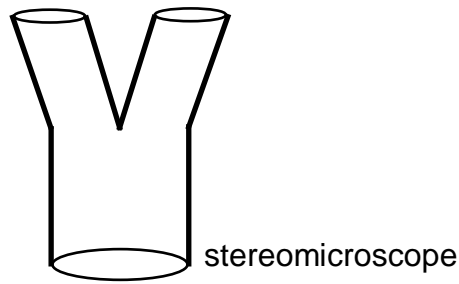


Fig. 7 Experimental apparatus for measuring the vacuum level achieved in chamber ch2 behind a short needle (the PLA) movable in the x, y, z direction within a plane aperture. PG1, PG2, PG3 and PG4 are pressure gauges for chambers ch1, ch2, ch3 and ch4, LV is a control gas inlet valve, RP is a mechanical rotary pump, and distance d is adjustable. Moving needle is viewable with stereo microscope.

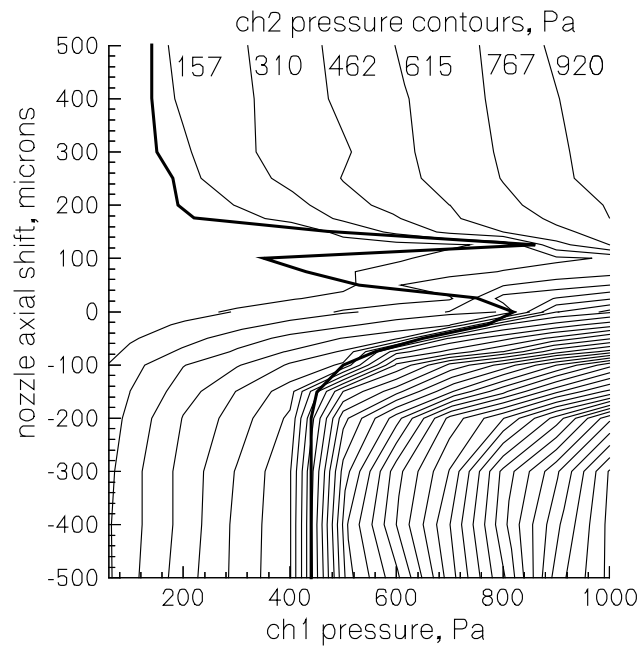


Fig. 8 Contours of constant ch2 pressure dependent on inner nozzle shift and ch1 pressure variables [ $p_2$  vs. (shift,  $p_1$ )]. Thick line shows points at sharp transition, or breakdown, of pumping action.

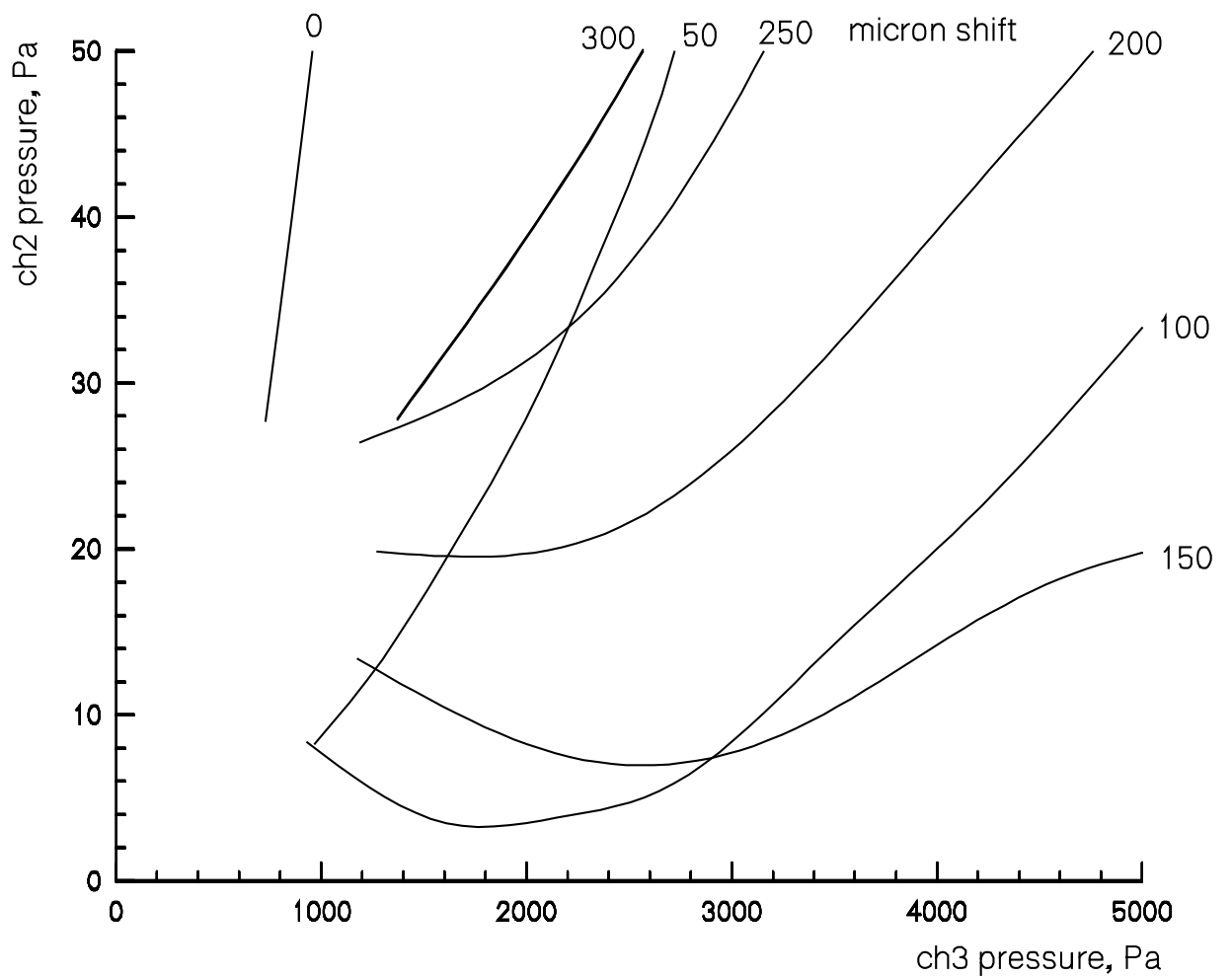


Fig. 9 Pressure in ch2 vs. pressure in ch3 at fixed nozzle shift in microns.



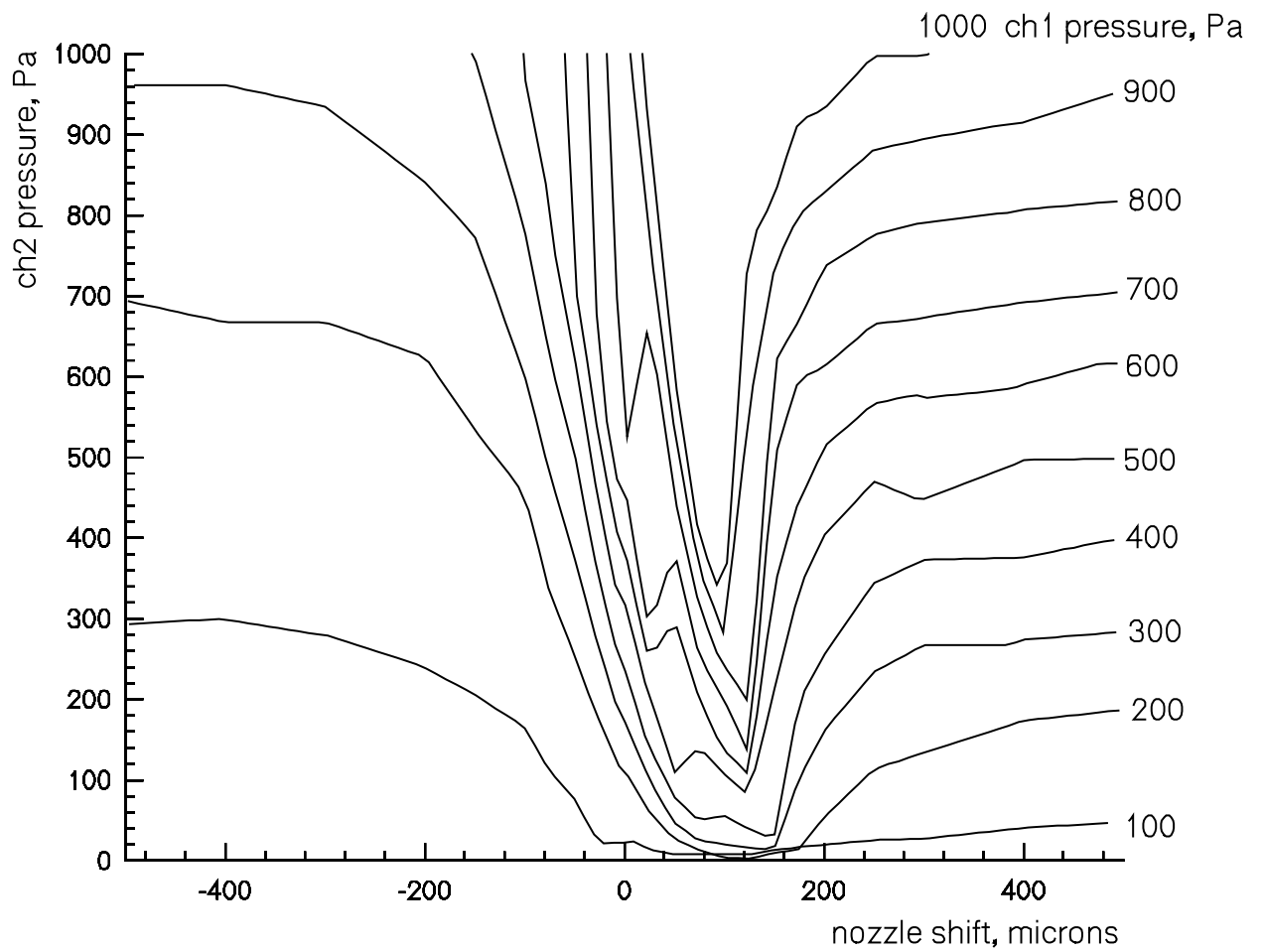


Fig. 10 Pressure in chamber ch2 vs. nozzle shift at fixed ch1 pressure.

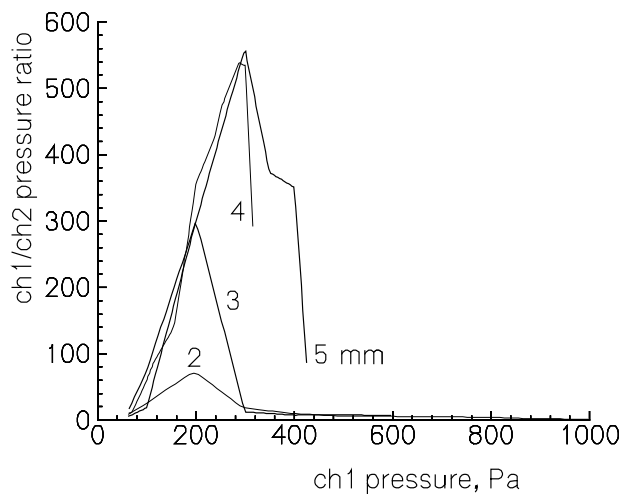


Fig. 11 ch1/ch2 pressure ratio vs. ch1 pressure at different baffle distance shown (in mm).

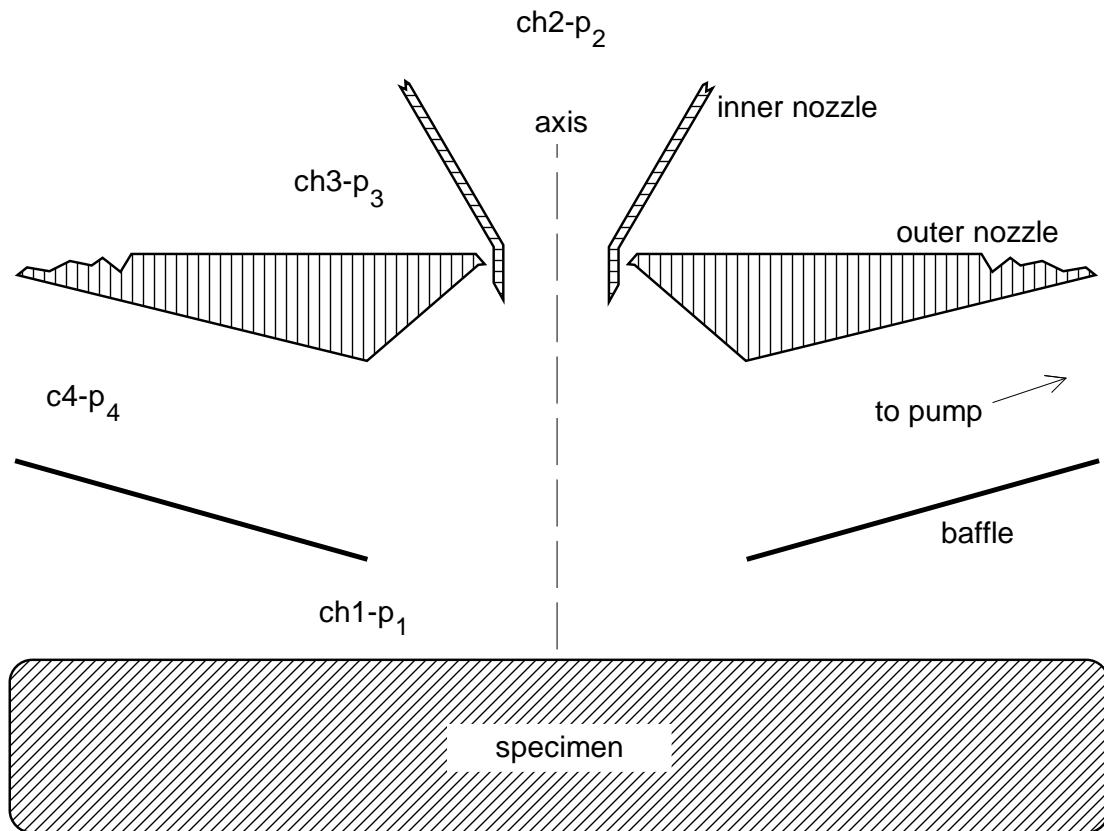


Fig. 12 Drawing of RF-PLA system with baffle and specimen corresponding to Fig. 6.